

# SPARC REANALYSIS INTERCOMPARISON PROJECT:

## CHAPTER 6: STRATOSPHERE-TROPOSPHERE COUPLING

Working Draft (September 7, 2014)

\* denotes confirmed action, as of summer 2014

### **Lead Authors**

Edwin P. Gerber\* (New York University, USA)

Yulia Zyulyaeva (P. P. Shirshov Institute Of Oceanology, Russia)

### **Contributing Authors**

Blanca Ayarzagüena (Freie Universität - Berlin, Germany)

David Barriopedro\* (Universidad Complutense de Madrid, Spain)

Mark P. Baldwin\* (University of Exeter, UK)

Thomas Birner\* (Colorado State University, USA)

Thomas J. Bracegirdle\* (British Antarctic Survey, UK)

Amy Butler\* (NOAA ESRL, USA)

Natalia Calvo\* (Universidad Complutense de Madrid, Spain)

Lesley Gray (University of Oxford, UK)

Steven Hardiman\* (Met Office, UK)

Peter Hitchcock\* (University of Cambridge, UK)

Maddalen Iza\* (Universidad Complutense de Madrid, Spain)

Alexey Karpechko (Finnish Meteorological Institute, Finland)

Kirstin Krueger (University of Oslo, Norway)

Ulrike Langematz\* (Freie Universität - Berlin, Germany)

Hua Lu\* (British Antarctic Survey, UK)

Gareth Marshall\* (British Antarctic Survey, UK)

Patrick Martineau\* (McGill University, Canada)

Daniel Mitchell (University of Oxford, UK)

Andrew Orr\* (British Antarctic Survey, UK)

Cristina Peña-Ortiz (University of Seville, Spain)

Seok-Woo Son\* (Seoul National University, Korea)

Masakazu Taguchi\* (Aichi University of Education, Japan)

## 1 Introduction

At this time, this document is only a skeleton of our chapter, where we have collected the active topics of research. For more information on the S-RIP project and the stratosphere-troposphere coupling chapter, see the following webpages.

S-RIP home page: <http://s-rip.ees.hokudai.ac.jp/>

Stratosphere-troposphere coupling chapter page:

[http://math.nyu.edu/~gerber/pages/strat-trop\\_coupling.html](http://math.nyu.edu/~gerber/pages/strat-trop_coupling.html)

## 2 Data Needs

Here I've tried to catalogue the data needs of various coauthors. Fortunately much of the zonal mean data will be made available to Patrick Martineau.

### Monthly means:

Zonal mean zonal wind, temperature, and EP flux. (Ideally all the data will be available on the same grid – this might be handled by Sean Davis.) *Do we want a standardized E-P flux data? Would want it at daily resolution or better.* Monthly mean geopotential height and SLP.

### Daily mean:

$\bar{u}, \bar{v}, \bar{T}, \bar{Z}, \overline{u'v'}, \overline{v'T'}$  on pressure levels (1000 to 30 hPa). Daily mean NAM and SAM indices (could be provided by Ed Gerber).

Daily gridded data (2.5x2.5 is enough) of: i) geopotential height at 500 hPa (Z500) and ii) of potential vorticity (PV) for the standard pressure levels between 500 and 150 hPa. Fields should be provided for the Northern Hemisphere and the full period of each reanalysis (although the cross-comparison of reanalyses would be confined to the same period).

Daily  $u$ ,  $v$ , and  $T$  are also requested – though analysis could be restricted to the 100 and 30 hPa levels. *Question: can one download single levels from the reanalysis centers, or does one need to get everything?*

Daily geopotential height at 1000 (for tracking surface signal) and 50 hPa (Z50) and 60N (to classify SSWs into wave number 1 and wave number 2 – if this classification is not standardized).

**4x daily:**  $u, v, w, t$  (This is from Patrick – I think he has access to all the data, but will provide everything in zonal mean format.)

**Central dates of SSWs** and their types (splitting and displacement) for each reanalysis. I believe that this could be provided by Amy Butler, though classifying into splits vs. displacement events is less trivial.

Note that Alfred-Wenger-Institute (AWI) have already calculated EP flux data for ERA-Interim, ERA-40, NCEP, and JRA ([http://www.awi.de/en/research/research\\_divisions/climate\\_science/atmospheric\\_circulations\\_old/projects/candidoz/ep\\_flux\\_data/](http://www.awi.de/en/research/research_divisions/climate_science/atmospheric_circulations_old/projects/candidoz/ep_flux_data/)).

### 3 Coupling on Synoptic to Intraseasonal Time Scales

This section will include analysis of SSWs, blocking, annular modes, planetary wave coupling, and wave-mean flow interactions. Here are the current contributions, in alphabetical order by author at this time.

#### 3.1 Characterizing Stratosphere-Troposphere Coupling associated with SSWs (Ayarzagüena and Langematz)

We propose two analyses for the chapter. Both of them concern stratospheric sudden warmings (SSWs), i.e., the coupling on synoptic to intraseasonal time scales

##### Main characteristics of SSWs

We plan to analyze the main characteristics of SSWs across all the reanalyses in order to assess the relevant dynamical processes associated with the occurrence and development of these phenomena in the different data sets. In particular, we will apply the diagnostic benchmarks proposed by Charlton and Polvani (2007) that include the study of the intensity, duration, deceleration of the zonal wind in the middle stratosphere associated with SSWs, the mean injection of wave activity preceding SSWs or the stratospheretroposphere coupling following these events (see the Table in Fig. 1). Charlton et al. (2007) applied the same metrics to assess the ability of different GCMs to reproduce the dynamics behind the occurrence of SSWs. In our case, we will follow the same statistical procedure to compare the results across the reanalyses. See Fig.2.

In a second step, we plan to compare these SSW-characteristics for SSWs identified with different criteria Butler et al. (2014). This might support the science community in the search of an appropriate diagnostic for the identification of SSWs.

##### Tropospheric forcing of SSWs

We plan to analyze the role of tropospheric forcing mechanisms in the occurrence of SSWs and to determine the sensitivity of the results to the different reanalysis data sets. For that purpose we will make use of the methodology proposed by Nishii et al. (2009) to analyze intraseasonal wave modulations. This methodology is based on the decomposition into a zonally-varying time-mean state and local departures from this time-mean state. For instance, the meridional eddy heat flux can be decomposed into different terms, which correspond to: the climatological planetary waves (first right-hand term of (1), the anomalous waves (second right-hand term) and the linear interaction between the climatological planetary waves and wave anomalies (third plus fourth term):

$$[v^*T^*] = [v_c^*T_c^*] + [v_a^*T_a^*] + [v_c^*T_a^*] + [v_a^*T_c^*] \quad (1)$$

where brackets and asterisks indicate zonal mean and deviation from it, respectively,  $v$  is the meridional wind,  $T$  is the temperature and the  $a$  and  $c$  subscripts denote anomalies and climatological values, respectively.

<b>SSW characteristics</b>	<b>Metrics</b>
Amplitude of SSW in the middle stratosphere (intensity)	Area-weighted mean 10-hPa polar cap temperature anomaly (90°-50°N) averaged $\pm 5$ days around the central date
Amplitude of SSW in the lower stratosphere (coupling between the middle and lower stratosphere)	Area-weighted mean 100-hPa polar cap temperature anomaly (90°-50°N) averaged $\pm 5$ days around the central date
Deceleration of the polar night jet	Difference in 10-hPa zonal-mean zonal wind at 60°N, 15-5 days prior to the onset date minus 0-5 days after the onset date
Wave activity prior to SSW	Area-weighted mean 100-hPa meridional eddy heat flux anomaly (45°-75°N), 20-0 days before the onset date
Stratosphere-troposphere coupling	RMS, area-weighted, 1000-hPa geopotential height anomaly, 20°-90°N, 10-60 days after the central date.

Figure 1: List of the dynamical benchmarks used for the characterization of the different processes related to SSWs (Charlton and Polvani, 2007).

This methodology will be applied to the meridional eddy heat flux to quantify the contribution of each term of the heat flux to the peak of wave activity preceding SSWs. The same methodology can be also used to determine the relative importance of these two components for the deceleration of the polar night jet associated with SSWs, when applied to the divergence of Eliassen-Palm flux as in Ayarzagüena et al. (2011).

We will carry out this analysis in two steps. First, we will study together all SSWs in each reanalysis and compare their results. As a second step, we will repeat the analysis, but considering separately vortex displacement SSWs and vortex split SSWs in the same way as Ayarzagüena et al. (2011) did for two cases of study (2009 and 2010 SSWs) (Fig. 2) and Smith and Kushner (2012) for SSWs for the period 1979-2009 (Fig. 3). Both studies used NCEP/NCAR reanalysis data and found a different predominant term in the peak of the heat flux prior to SSWs for vortex displacement SSWs and vortex split SSWs: linear interference between climatological and anomalous waves for the former and wave activity associated with wave anomalies themselves for the latter.

**Concerns:** The comparison of the results between split SSWs and displacement SSWs can be very sensitive to the algorithm used for the classification of these two types of events. However, we think that it would be interesting to verify if all reanalyses show the same differences in the triggering mechanisms between split and displacement SSWs as in NCEP/NCAR reanalysis.

Also, this analysis is data intensive. Apart from the central dates of SSWs and their classification

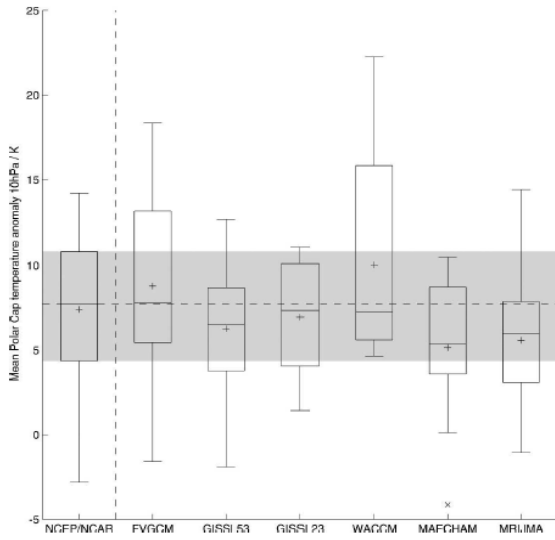


FIG. 4. Box plots showing distribution of maximum polar cap temperatures at 10 hPa ( $90^{\circ}$ – $50^{\circ}$ N) for SSW in a range of GCMs and NCEP–NCAR reanalysis. Gray shading shows interquartile range of reanalysis; dashed black line shows median of reanalysis. Outliers are marked by “x.” Mean is shown by a cross.

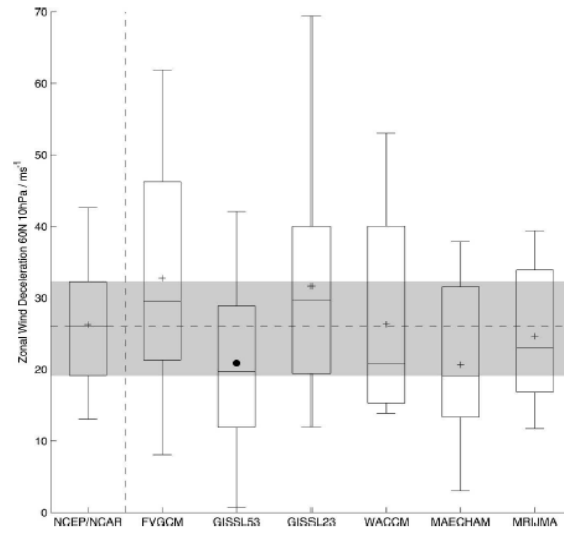
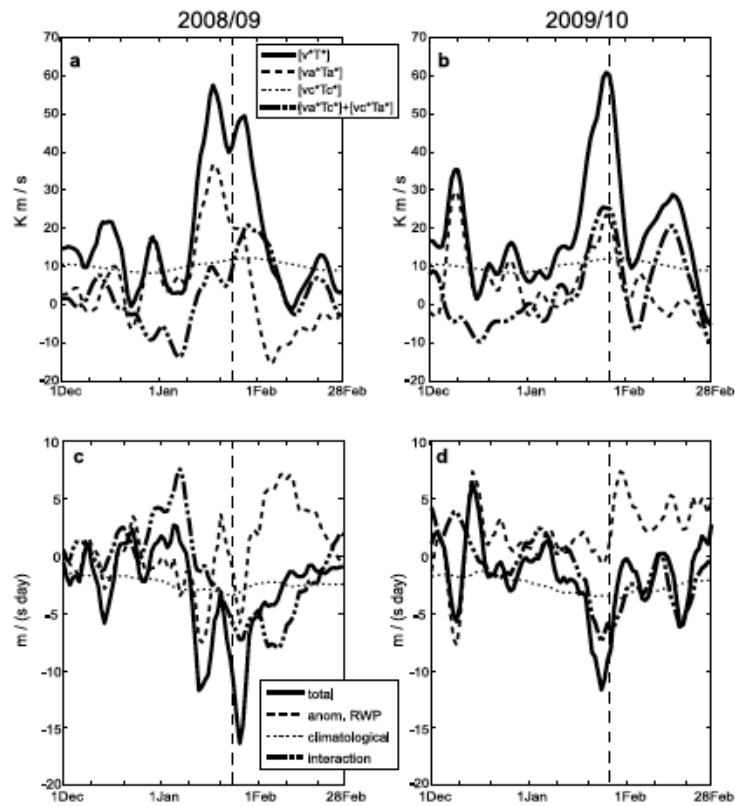


FIG. 6. Same as in Fig. 5, but for mean zonal wind deceleration at  $60^{\circ}$ N and 10 hPa.

Figure 2: These plots are taken from Charlton et al. (2007) for two different diagnostic benchmarks of SSWs: (left) the intensity of SSWs and (right) the deceleration of the polar night jet associated with SSWs. We will produce similar plots for each metric of Table 1, but instead of comparing different GCMs, we will use different reanalyses.

into vortex displacement SSWs and vortex split SSWs, we would need daily (non-zonal mean) data of  $u$ ,  $v$  and  $T$  at pressure levels from 850 hPa to the stratosphere (at least 30 hPa). Due to the huge amount of data, we could restrict the analysis to 100 and 30-hPa levels, but then the performance of the Smith and Kushner-like analysis will be limited.



**Figure 4.** (a) Time evolution of zonal-mean meridional eddy heat flux averaged over 50°N–80°N ( $\text{K ms}^{-1}$ ) at 100 hPa from 1 December 2008 to 28 February 2009. The different lines indicate total flux (solid line) and its contributions: the climatological-mean planetary waves (dotted line), the anomalies associated with Rossby wave packets (RWP) (dashed line), and the interaction between these anomalies and the climatological planetary waves (dash–solid line). The vertical line indicates the central date of the MSW. (b) Same as Figure 4a but for 2009/2010. (c and d) Same as Figures 4a and 4b but for the divergence of Eliassen-Palm flux ( $\text{ms}^{-1} \text{d}^{-1}$ ) at 10 hPa and 60°N.

Figure 3: This figure is taken from Ayarzagüena et al. (2011). We will compute composites of these magnitudes for all SSWs in each reanalysis.

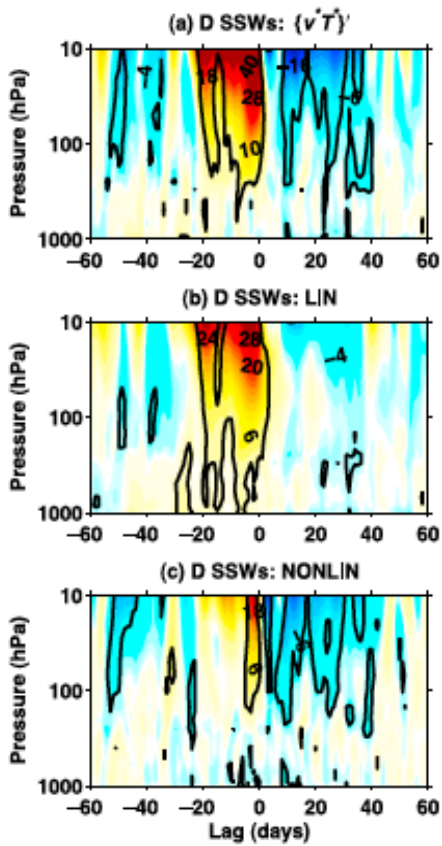


**Figure 7.** Composite mean daily heat flux anomaly decomposition for Displacement (D) SSWs. (a)  $\{v^*T^*\}'$ , (b) LIN and (c) NONLIN. Contour interval is  $2 \text{ mKs}^{-1}$ . Black contour indicates pressures and times for which the composite mean is different from zero at the 95% significance level.

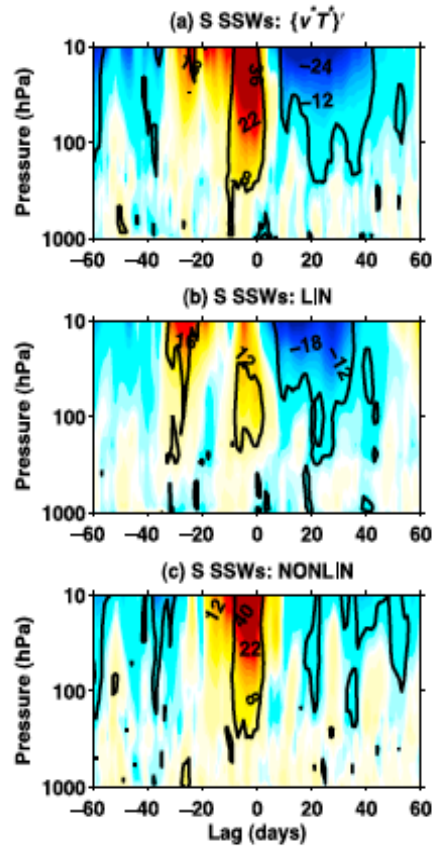


**Figure 8.** Composite mean daily heat flux anomaly decomposition for Split (S) SSWs. (a)  $\{v^*T^*\}'$ , (b) LIN and (c) NONLIN. Contour interval is  $2 \text{ mKs}^{-1}$ . Black contour indicates pressures and times for which the composite mean is different from zero at the 95% significance level.

Figure 4: These figures are taken from Smith and Kushner (2012). We will carry out the same analysis for all reanalyses.

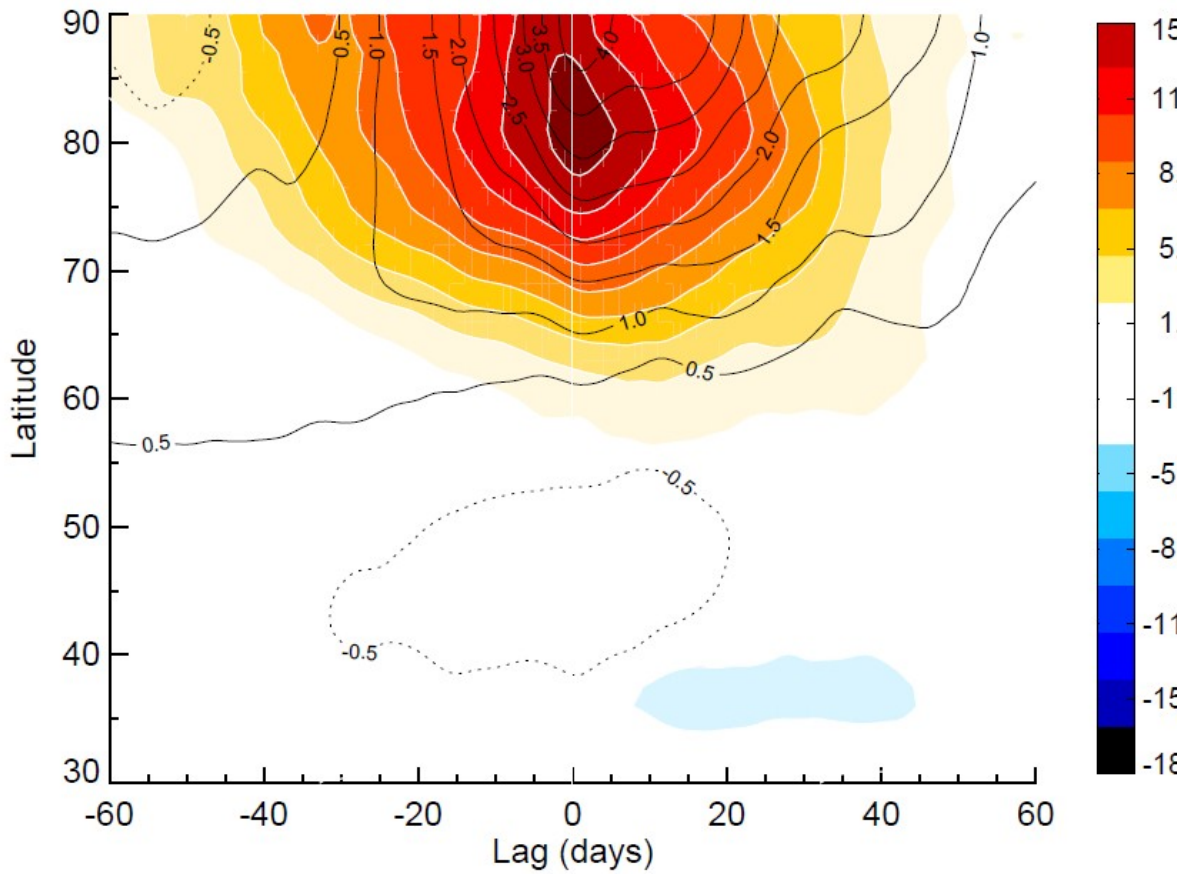


Figure 5: Regressions on the PV530K index as a function of latitude, during JanMar, in ERA-Interim data. Colors: anomalous dynamical (PV=2) tropopause pressure; black contours: anomalous surface pressure.

### 3.2 PV based analysis of S-T Coupling (Birner and Baldwin)

Analysis along the lines of Baldwin and Birner (in preparation); see Fig. 5, based on ERA-intrim. It would be fairly simple to run for other data sets (only zonal mean quantities required, but at daily resolution).

### 3.3 Blocking patterns associated to SSWs and the modulation of ENSO (Barriopedro and Calvo)

To describe the links between blocking and SSWs (or other metrics that can be used to diagnose strongly perturbed polar vortex states, such as NAM) and the sensitivity of the results to the reanalysis used.

We will follow the work of Barriopedro and Calvo (2014) to address:

1. The spatial patterns of the blocking precursors of SSWs in different reanalyses (as in Fig. 6).
2. The role of ENSO in modulating the blocking-SSWs links described above. We could also explore changes in the blocking patterns with respect to the type of SSW (either splitting and displacement or wave number 1 and wave number 2, see Fig. 6).
3. Depending on time and data availability, we could also explore the sensitivity of the above results to the blocking definition (see Barriopedro et al. (2010) for a review of blocking methods).

**Concerns:** We do not expect large differences in the blocking climatology between reanalyses, and that is why we would focus on a small subset of blocking events (blocking precursors of SSWs). For the proposed analyses, there could be substantial discrepancies between blocking definitions.

The standard data used in most previous publications relating blocking and SSW is daily gridded PV in standard pressure levels between 500 and 150 hPa, e.g., Martius et al. (2009) and Barriopedro and Calvo (2014). ENSO events would be identified from already observational indices (CPC NOAA), so no additional data from the reanalysis should be required. This would require a tremendous amount of analysis, and a simpler definition will be needed.

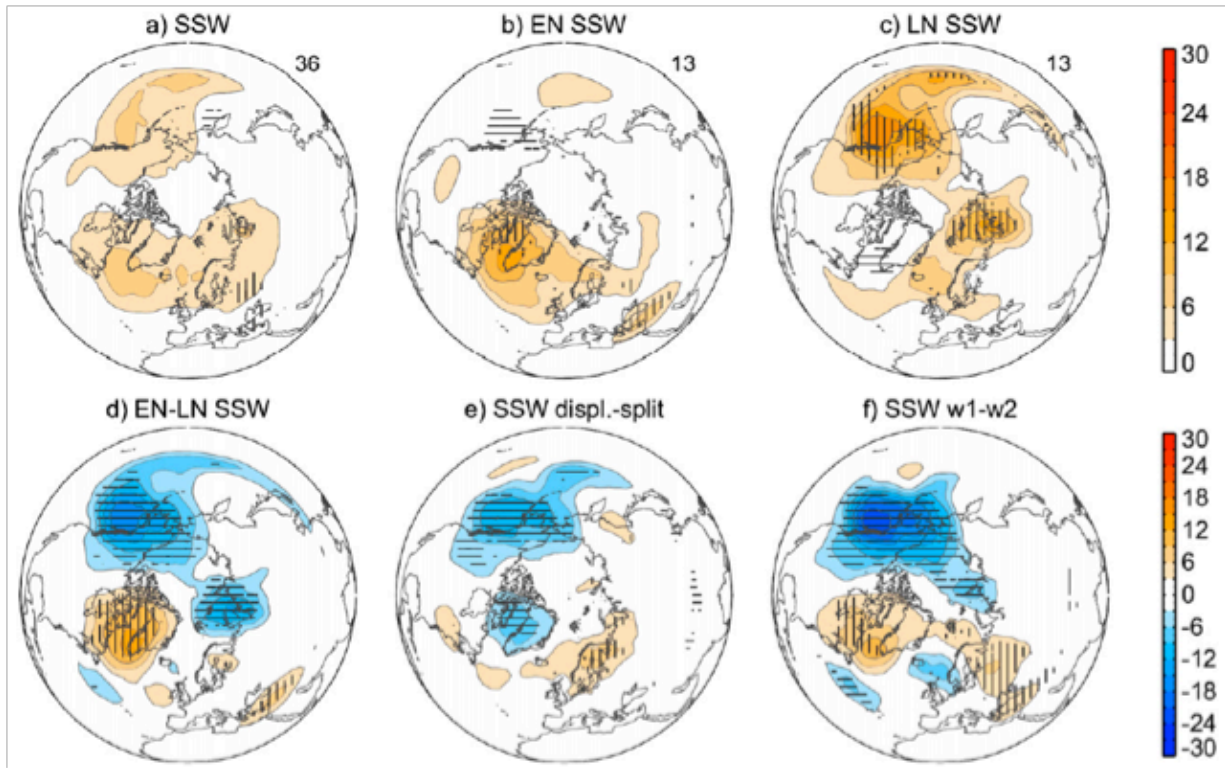


Figure 6: (From Barriopedro and Calvo 2014.) Composites of blocking precursors of SSWs for (a) all, (b) EN, (c) LN winters, and the composite difference of the blocking precursors for (d) EN minus LN SSWs, (e) displacement minus splitting SSWs, and (f) wave-1 minus wave-2 SSWs. Blocking precursors are identified from the blocking frequency for the  $[-10, 0]$ -day period before the central date of SSWs. The blocking frequency is expressed as the percentage of time (over the 11-day period) during which a blocking was detected at each grid point. Vertical (horizontal) hatched areas indicate regions with blocking activity significantly above (below) climatology at the 95% confidence level.

### **3.4 Stratospheric Sudden Warmings (Butler)**

I will construct a table that shows the different SSW dates in different reanalyses, and/or something like Fig. 7 (from Butler et al. (2014)), but updated to include different reanalyses instead of just NNR.

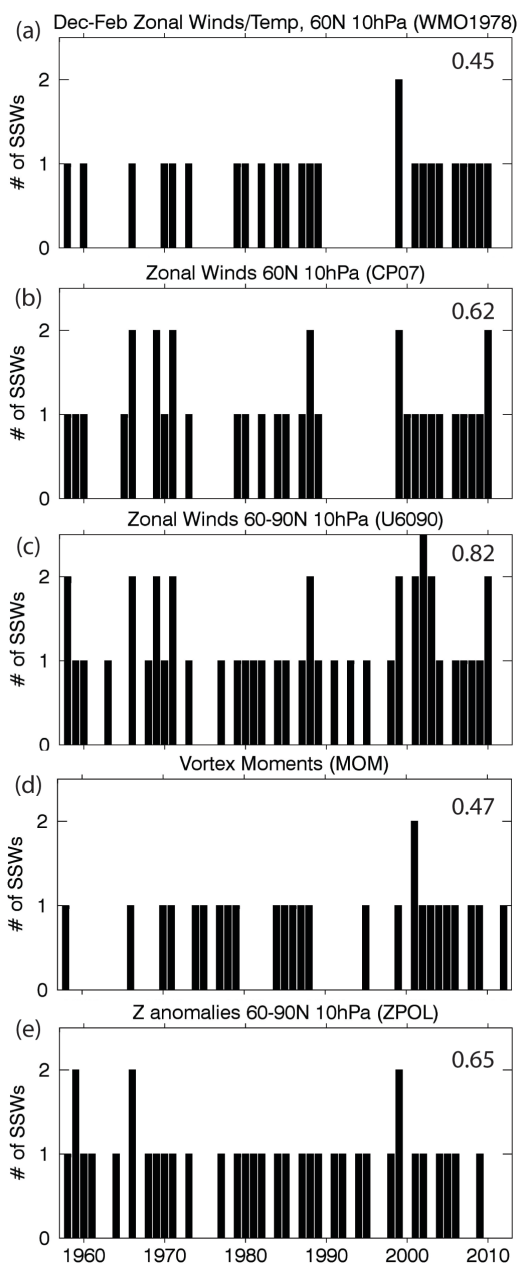


Figure 7: Time series (using NCEP-NCAR reanalysis from 1958-2012) of major mid- winter SSWs as defined using five different diagnostics (described in Table 1 of Butler et al. (2014)): (a) zonal-mean zonal winds at 60N and 10 hPa, Dec-Feb only, and a temperature gradient reversal; (b) zonal-mean zonal winds at 60N and 10 hPa, following guidelines by Charlton and Polvani (2007); (c) zonal-mean zonal winds at 10 hPa and averaged from 60- 90N, following guidelines by Charlton and Polvani (2007); (d) vortex moment diagnostics; and (e) geopotential height (Z) anomalies averaged from 60-90N at 10 hPa, exceeding 3 standard deviations of the JFM mean climatology. The abbreviations correspond to those in Table 1. The average number of SSWs per winter is given in the upper right corner of each panel (corresponding values for ECMWF reanalysis given in Table 1).

### 3.5 Stratosphere-troposphere coupling as revealed by the annular modes (Gerber)

I plan to analyze the zonal mean variability of the troposphere-stratosphere system, focussing on the annular modes which quantify the strength of the stratospheric polar vortex and position of the tropospheric jet stream, respectively. The goal will be to assess the spatial and temporal structure of the annular modes across all the reanalyses. Following Gerber et al. (2010), we'll focus on:

1. The spatial structure of the annular mode (e.g. Fig 8 – which is just Fig. 5 and 6 from Gerber et al. (2010) – but focussing on different reanalyses instead of models.
2. The seasonality of the variance, time scales, and stratosphere-troposphere lagged coupling (e.g. Fig. 2 below, which shows analysis of ERA-40 / ERA-Interim).
3. The dripping paint coupling between the troposphere and stratosphere (e.g Baldwin and Dunkerton, 2001). (This result is easy to compute, once one has the annular mode indices needed for 1 and 2.)

**Concerns:** Uncertainty in these metrics may be dominated by the finite length of the data records, not uncertainties in the reanalyses. Careful analysis will be needed to determine whether there are any significant differences between the reanalyses. The length of the comparison period will be critical hence a problem with ERA-40 that stops early.

References: Thompson and Wallace (2000); Baldwin and Dunkerton (2001); Baldwin et al. (2003); Gerber et al. (2010).

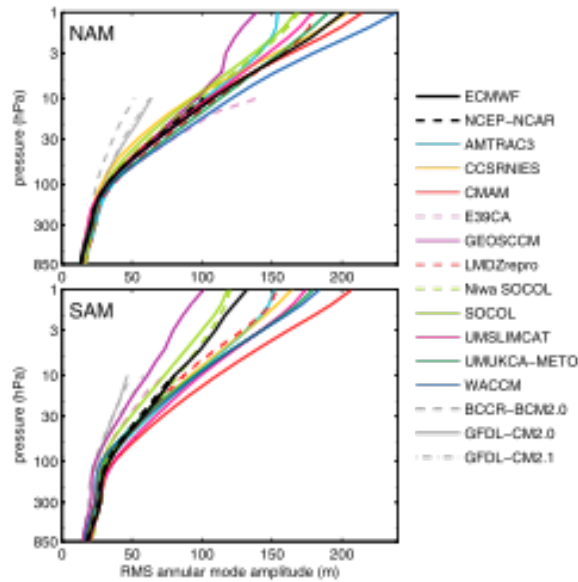


**Figure 5.** The root mean square amplitude of the annular mode pattern of variability in the CCMs as a function of pressure in the (top) NH and (bottom) SH. Analysis of the reanalyses and three IPCC-AR4 models are included for reference, and marked with black and gray lines, respectively.

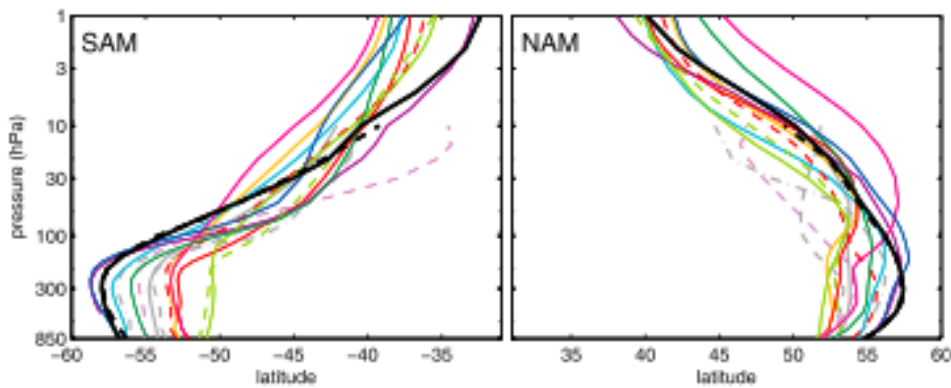


**Figure 6.** The latitude of the node of the annular mode patterns of variability as a function of pressure. Line colors correspond to the legend in Figure 5: thick black lines are based on ECMWF and NCEP-NCAR reanalyses, thin-colored lines are based on the CCMs, and gray lines are based on the IPCC-AR4 models. Note the significant latitude bias in the troposphere of both hemispheres, which reflects the fact that the tropospheric jet stream is too far equatorward in most models.

Figure 8: These figures were ripped from Gerber et al. (2010). Well do this type of analysis on all the reanalyses. Do they differ as much as different models?

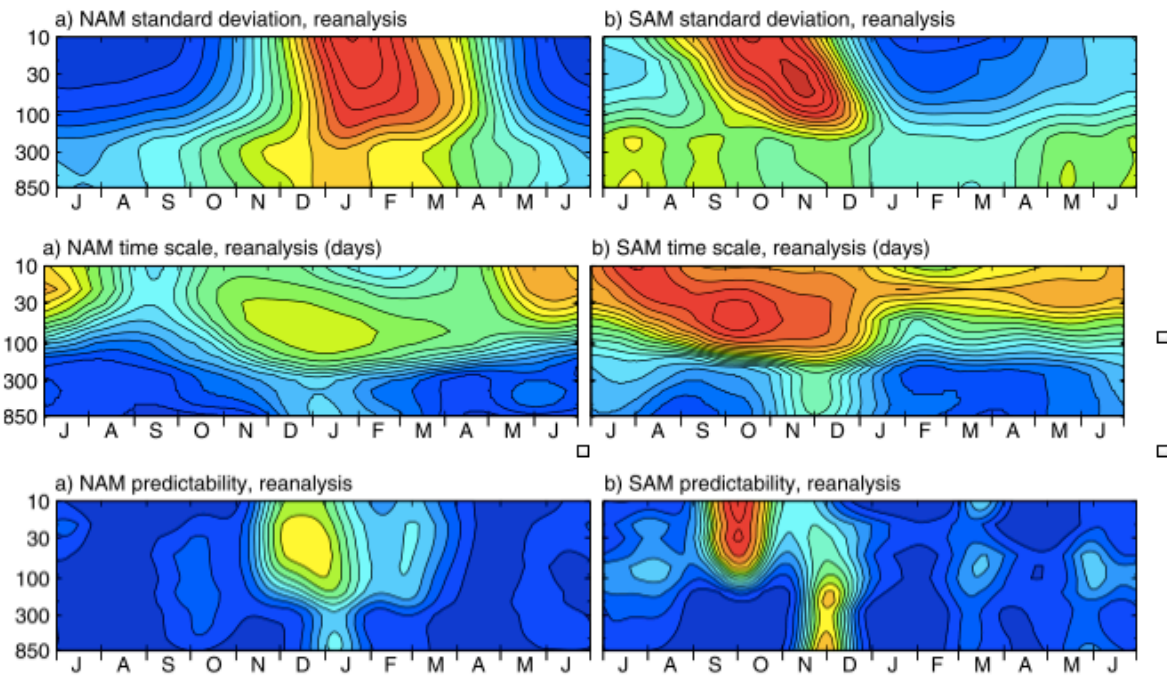


Figure 9: These plots were culled from Gerber et al. 2010, Figs. 7-9. The results are based on ERA-40 + ERA interim. We'll repeat this for all the reanalyses. To avoid overwhelming the reader, I'll have to find a more compact way of showing this information.

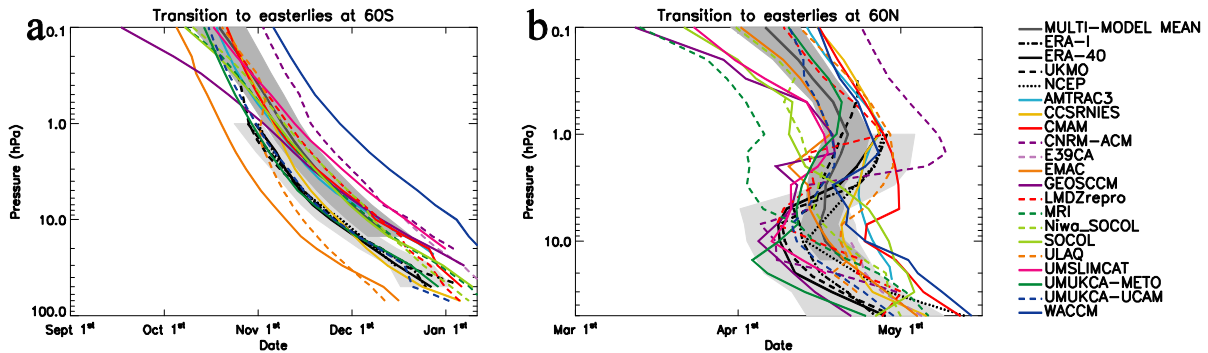


Figure 10: Final transition of zonal mean zonal wind from westerly to easterly at (a) 60S and (b) 60N. CCMVal-2 monthly mean model data is used (from 1980/1999), with each model represented by a coloured line and the multimodel mean shown as a dark gray line. The dark gray shading indicates the inter-model standard error, scaled to represent a 95% confidence interval. ERA-Interim (1989/2009), ERA-40 (1980/2002), and NCEP (1980/1999) reanalysis and UKMO analysis data (1992/2001) are shown as black dot-dashed, solid, dotted and dashed lines respectively, with light gray shading indicating the interannual standard deviation in the ERA-Interim data, again scaled to represent a 95% confidence interval. From Hardiman et al. (2011).

### 3.6 Final warmings in the Southern and Northern Hemispheres (Hardiman)

The final warming of the polar vortex is of key importance in chemistry-climate models since, once the polar vortex has broken down, ozone rich air can be transported to polar latitudes again. A bias in the final warming time is also an indication of polar temperature biases, which will adversely affect the modelling of heterogeneous ozone destruction there. Furthermore, strong stratosphere-troposphere coupling takes place during the final warming, with an influence on the North Atlantic Oscillation and Southern Annular Mode, and thus the timing of the final warming has implications for seasonal forecasting.

The final warming date is defined here as the day on which the zonal mean zonal wind at 60 becomes easterly for the final time during winter/spring. This can be sufficiently diagnosed using monthly mean data (calculating the day of the final warming using linear interpolation and assuming the monthly mean value represents the value on day 15 of the month), and occurs first in the mesosphere in the southern hemisphere but first in the mid-stratosphere in the northern hemisphere (Fig. 10).

A closer study of the final warming in the northern hemisphere reveals that in some years the final warming occurs first in the mid-stratosphere (10hPa-first years), and in some years occurs first in the mesosphere (1hPa-first years), as shown in Fig. 11. Correctly predicting the final warming type has the potential to add skill to seasonal forecasts in the northern hemisphere spring Hardiman et al. (2011). In ERA-Interim 81% of years are 10 hPa-first years, whereas only

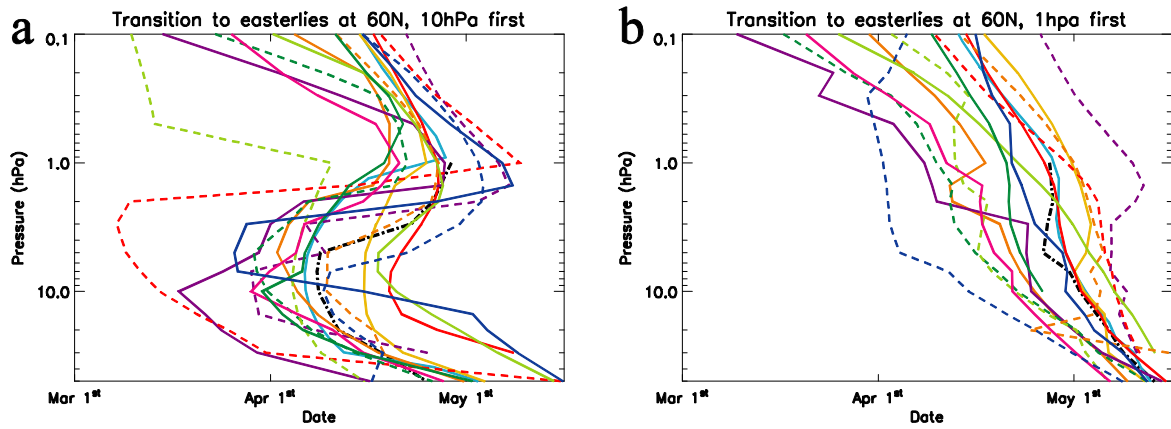


Figure 11: Mean final warming date at 60N composited over (a) 10 hPa-first years and (b) 1 hPa-first years (defined in text), calculated from CCMVal-2 model data (coloured lines) and ERA-Interim (black line). From Hardiman et al. (2011).

36% of all modeled years (using the CCMVal-2 models) are 10 hPa-first years.

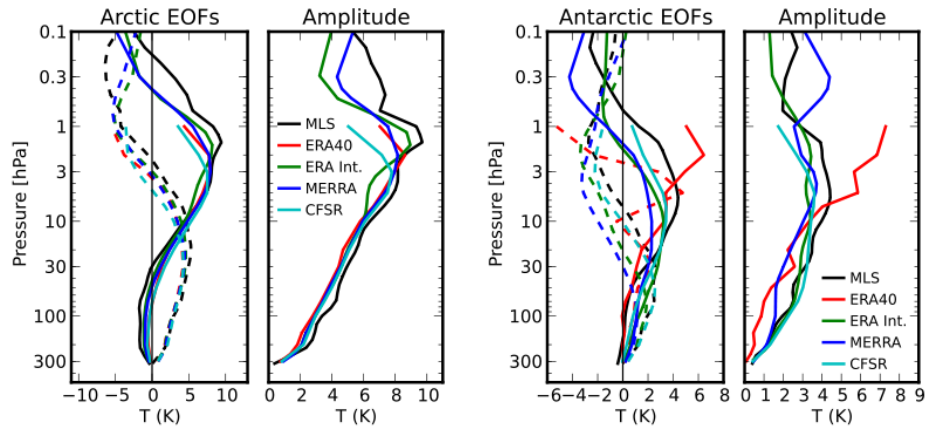


Figure 12: First and second EOF of polar-cap averaged temperatures from selected reanalyses for northern hemisphere (left) and southern hemisphere (right).

### 3.7 The vertical structure of polar cap variability (Hitchcock)

I would like to evaluate the variability of polar-cap averaged stratospheric temperatures, with an emphasis on the first two modes of variability as defined by an EOF analysis, after Hitchcock et al. (2013). The first part of this will involve evaluating whether the EOF analysis captures the same variability in each reanalysis product, e.g. Fig. 12. This is not the case in the SH according to some preliminary work, although the analysis is complicated by the larger trends in the SH. Then, I'll subsequently identifying (if possible) a single best pair of vertical modes that capture the physical variability.

Once I have this best estimate, I would like to project the variability in each reanalysis onto these modes to construct 'abacus' plots, again after Hitchcock et al. (2013), as shown in Fig. 13. I am particularly interested in evaluating (a) pre-1979 variability in the northern hemisphere and (b) southern hemisphere variability. Finally, the abacus plots have been useful in comparing and displaying the dates of other event-based metrics; if this is useful for other authors' work in this chapter this could be done as well.

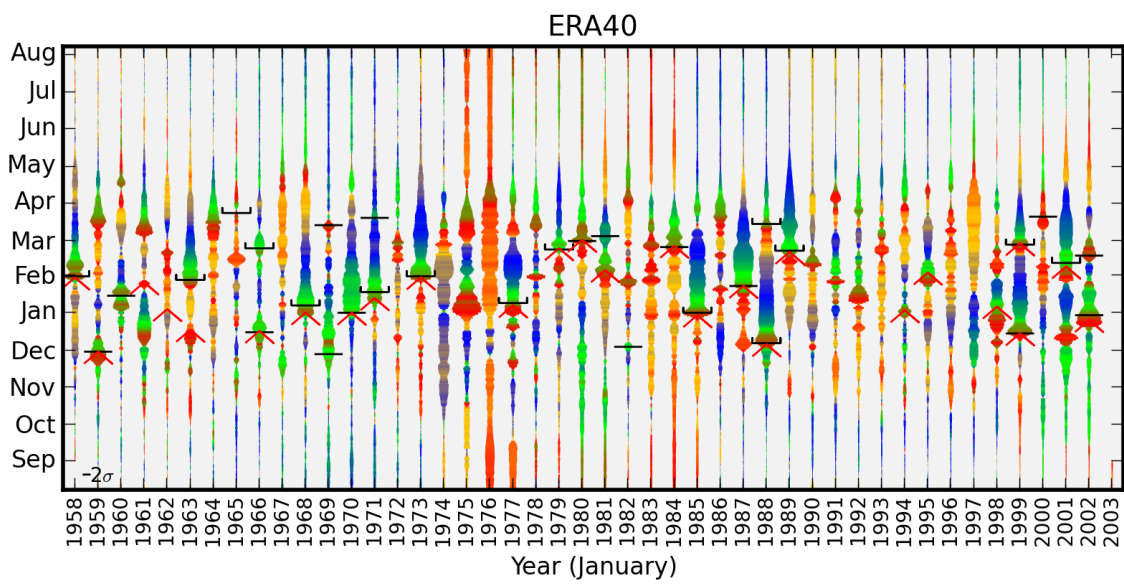


Figure 13: Abacus plot of ERA40 showing split and displacement sudden warmings, after Charlton and Polvani (2007).

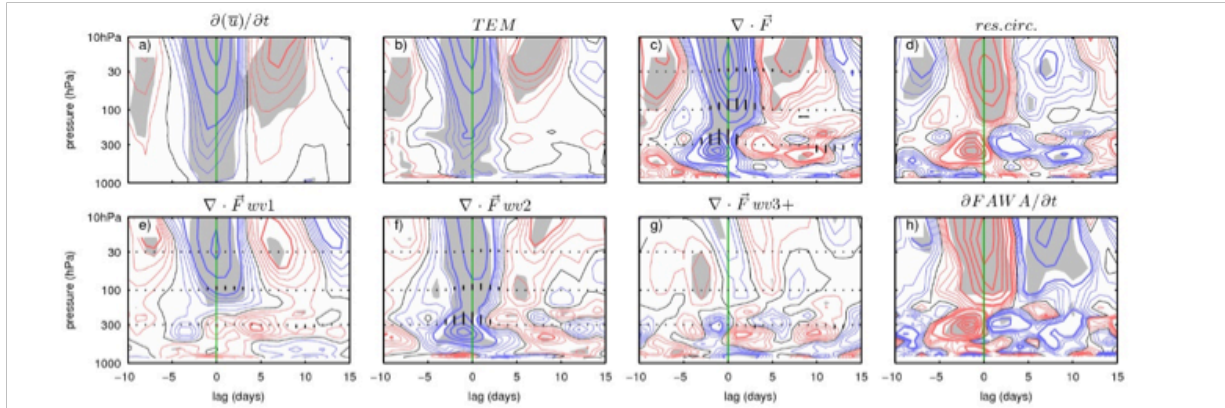


FIG. 2. TEM diagnostic evolution of composite SVW events. All quantities shown are averaged over  $50\text{--}90^\circ\text{N}$ . Zonal wind tendency and terms from the TEM equation are shown with contour interval of  $0.20 \text{ ms}^{-1}\text{day}^{-1}$  as fine contours and of  $1 \text{ ms}^{-1}\text{day}^{-1}$  as coarse contours. Vertical component of EP flux is shown with arrows on the 300, 100 and 50 hPa levels with the distance from 300 to 100 hPa equivalent to  $3.5 \times 10^6 \text{ m}^2\text{s}^{-1}\text{Pa}$  of  $\vec{F}_p$ . FAWA tendency is shown in h) with same contours as wind tendency. Statistical significance is shown with gray shading. Significant EP fluxes are denoted with thick black arrow.

Figure 14: TEM Diagnostics from Martineau and Son (2014); I suggest showing panel a) c) d) and h) for all reanalyses. Only Era-Interim is used in current figure.

### 3.8 Stratosphere-Troposphere Coupling during Stratospheric Vortex Weakening (SVW) events: evolution of zonal-wind and wave activity in the extratropics (Martineau and Son)

I plan to analyze zonal-mean wind variability and wave activity in the troposphere-stratosphere coupled system during events of strong stratospheric zonal-wind deceleration. The goal is to assess the consistency of zonal-wind and wave activity across reanalyses in the context of strong wave-mean flow interaction events, examples shown in Figs. 14 and 15. We will focus on:

1. Temporal evolution of polar zonal wind and wave forcing diagnostics during SVW events.
2. Latitudinal structure of zonal wind tendency and forcing.

**Concerns:** Diagnostics of wave forcing and wave activity are likely sensitive to the numerical resolution. Interpolation to a common grid might be necessary before performing the diagnostics.

References: Nakamura and Solomon (2011); Martineau and Son (2013, 2014)

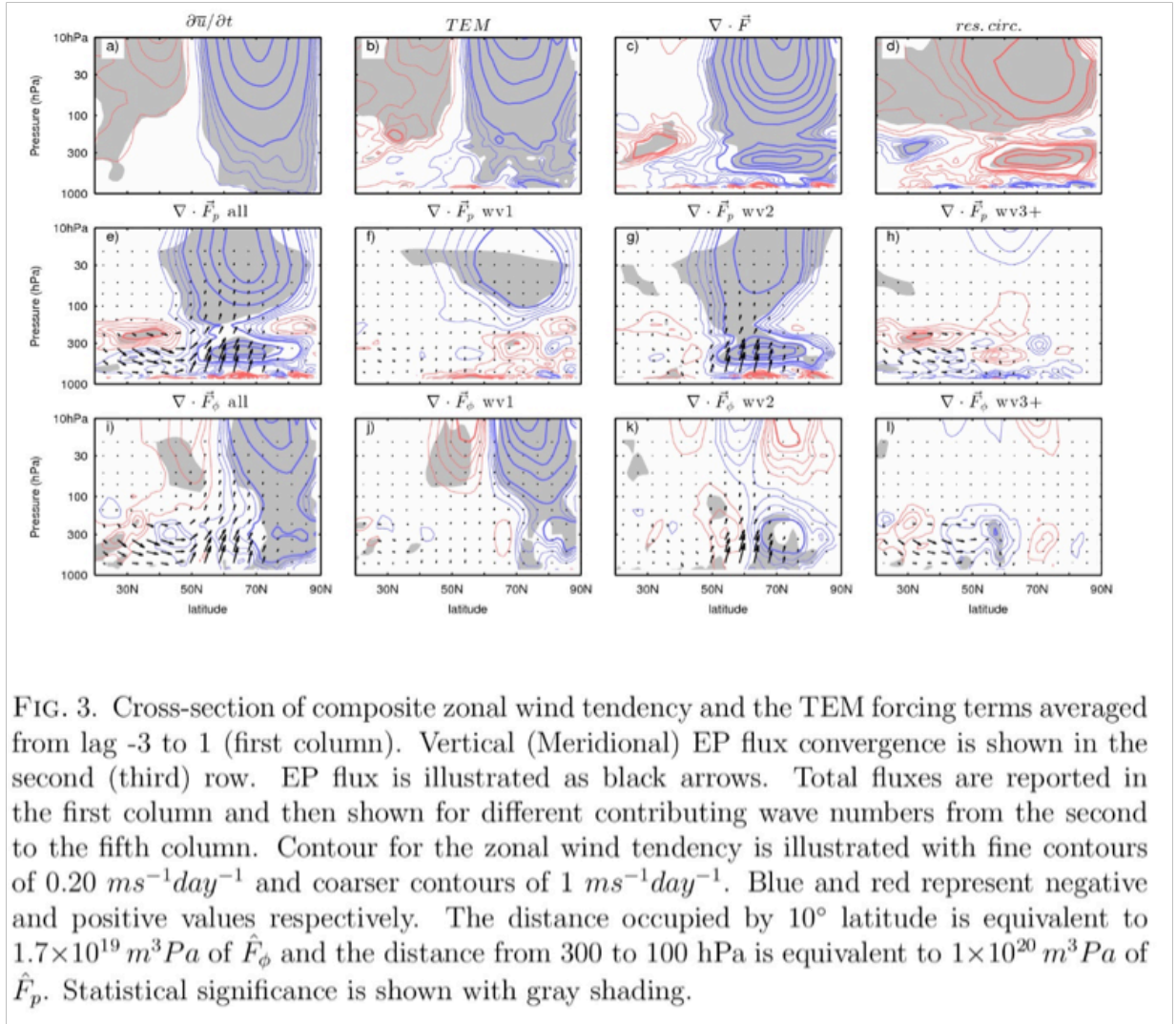


Figure 15: TEM Diagnostics from Martineau and Son (2014); I suggest showing panel a) c) d) for all reanalyses. EP flux can be displayed on panel c. Only ERA-Interim is shown here.

### 3.9 Extreme events (Son)

Temporal variability of stratospheric extreme events; quantile regression will be applied to stratospheric SAM and NAM. This will be linked with the analysis of Gerber above. See Fig. 23.

**General Bibliography** (in no particular order): Thompson et al. (2006); Song and Robinson (2004); Thompson and Birner (2012); Baldwin and Birner (2013); Butchart et al. (2011); Baldwin and Dunkerton (1999); Mitchell et al. (2011, 2013); Frame and Gray (2010); Driscoll et al. (2012); Limpasuvan et al. (2004); Newman et al. (2001)

## **4 Coupling on Intraseasonal to Interannual Time Scales**

The impact of Volcanoes, ENSO, QBO (to be coordinated w/QBO chapter), and Solar Cycle on stratosphere-troposphere coupling.

### **4.1 Troposphere-stratosphere coupling through ENSO (Calvo and Iza)**

Goal: To describe the bottom-up and top-down pathways of the ENSO signal between the troposphere and the stratosphere.

We plan to analyze the ENSO signal in the stratosphere in tropics and high latitudes. We will focus on zonal mean zonal wind and temperature responses to Eastern Pacific and Central Pacific ENSO following the studies by García-Herrera et al. (2006); Calvo et al. (2010); Zubiaurre and Calvo (2012). (See e.g. Fig. 16.)

We will also analyze the downward propagation of the polar signals from the stratosphere back to the troposphere (as in Manzini et al. (2006); Cagnazzo and Manzini (2009); Ineson and Scaife (2009), etc. Figs. 17 and 18) and possibly the differences in the signals during winters with and without SSWs (following Iza and Calvo, in preparation).

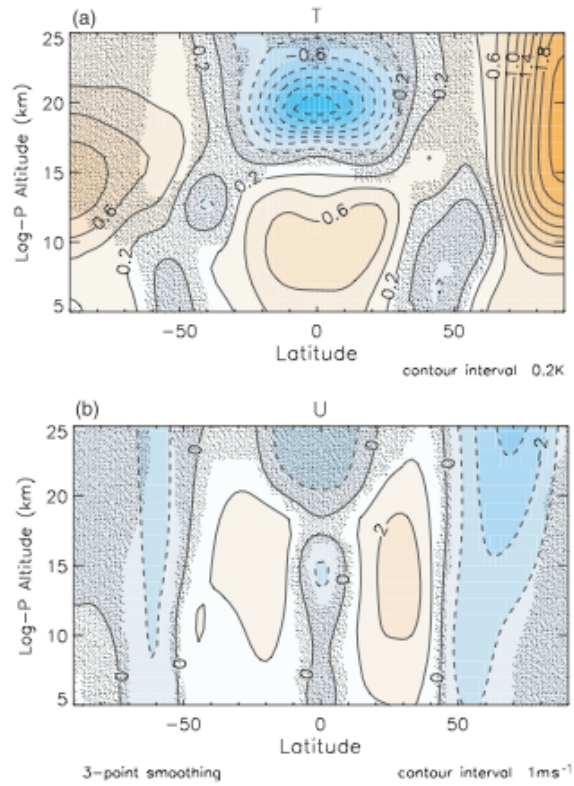
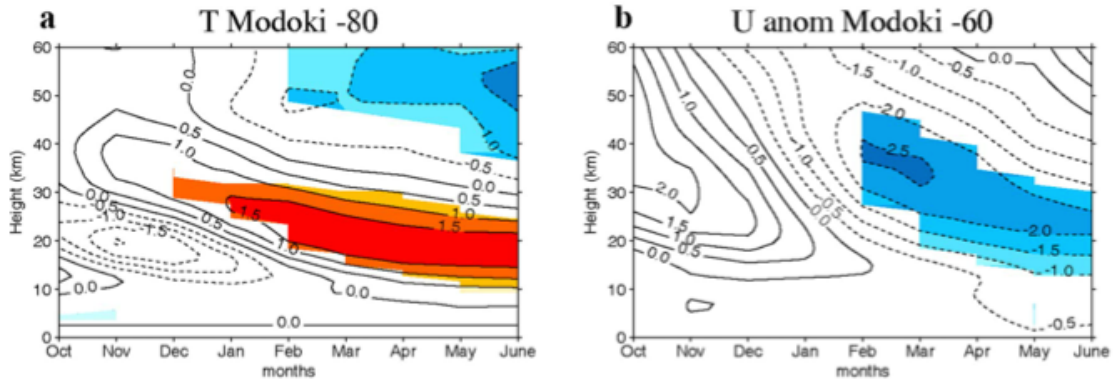


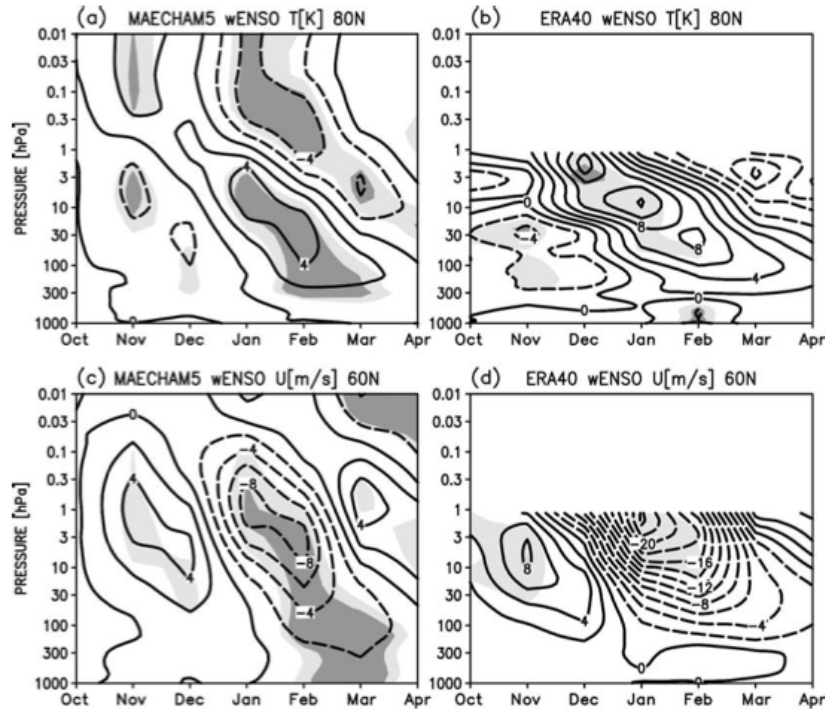
FIG. 4. As in Fig. 1a, but for (a) zonal-mean temperature and (b) zonal wind anomalies for the warm ENSO events. Contours are drawn every 0.2 K for temperature and 1 m s<sup>-1</sup> for zonal winds.

Figure 16: (From Calvo et al. JAS 2010): warm ENSO composite for (a) zonal mean temperature and (b) zonal mean zonal wind anomalies.



**Figure 5.** October–June composites of zonal mean temperature anomalies at (a) 80°S (contours drawn every 0.5 K) and (b) zonal mean zonal wind anomalies at 60°S for El Niño Modoki events (contours drawn every 0.5 m s<sup>-1</sup>). Colored regions are significant at the 95% level according to a Monte Carlo test.

Figure 17: From Zubiaurre and Calvo (2012).



**FIG. 4.** October–April monthly zonal-mean w ENSO anomaly. Temperature (contour: 2 K) at 80°N for (a) the ensemble of simulations and (b) the ERA-40 data. Zonal wind (contour: 2 m s<sup>-1</sup>) at 60°N for (c) the ensemble of simulations and (d) the ERA-40 data. Light and dark shades indicate statistical significance at the 95% and 99% levels, respectively.

Figure 18: From Manzini et al. (2006).

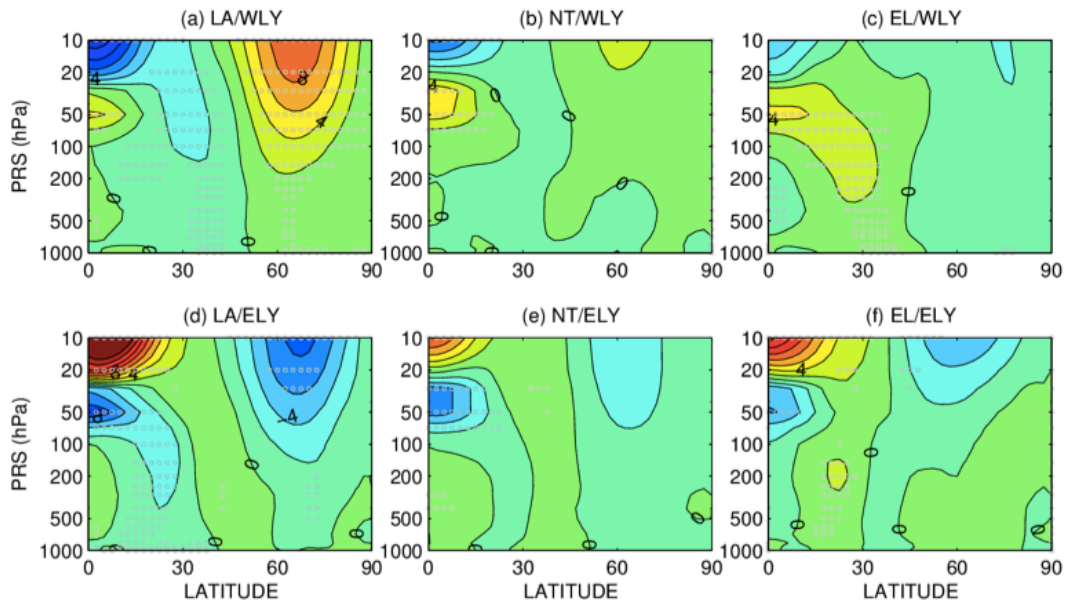


Figure 1: Latitude-height sections of DJF zonal mean zonal wind differences (m/s) for the six groups (as indicated in the title) from the climatology. This result is based on the NCEP/NCAR reanalysis data for 1957/58 to 2012/13 and taken from Taguchi (2014).

Figure 19: Zonal Wind Diagnostics (Taguchi)

## 4.2 ENSO and QBO connections to NH (Taguchi)

I plan to examine interannual changes in the NH winter extratropical stratosphere with ENSO and QBO, as existing studies suggest nonlinear changes with the two factors. We will look at changes in the zonal mean zonal wind and EP flux to examine how these changes occur consistently in response to ENSO and QBO. An example of the analysis is shown in Fig. 19.

**Concerns:** A preliminary analysis shows that the changes in the zonal mean zonal wind and EP flux with ENSO and QBO are similar among the different reanalysis datasets (except for NCEP20CR). If this is not interesting, then I think it might be better to extend the analysis to a more general picture of interannual variability of a few key quantities.

References: Garfinkel and Hartmann (2007); Wei et al. (2007); Calvo et al. (2009) and Taguchi (2014, JMSJ, in revision).

**General bibliography:** Crooks and Gray (2005); Charlton-Perez et al. (2013); Lu et al. (2013); Seppälä et al. (2013); Cnossen et al. (2011); Lu et al. (2009); Ho et al. (2009); Karpechko et al. (2010b)

## 5 Coupling on Interdecadal Time Scales and Longer

Coupling to meridional overturning circulation of the ocean(?), and the impact of stratospheric ozone loss and other forcings (water vapor?) on tropospheric trends.

### 5.1 Stratosphere-troposphere coupling associated with the Antarctic ozone hole: A comparison of reanalyses (Orr, Bracegirdle, Lu, and Marshall)

We plan to analyse the representation of Southern Hemisphere circulation/temperature changes and wave-driving associated with the Antarctic ozone hole in different reanalyses. The analysis will focus on circulation changes (e.g. 1 below) and the dynamical mechanism and wave driving (2-4 below).

1. Comparison of zonally averaged plots of trends in the zonal wind, temperature and geopotential height at 65S as a function of pressure and time. This is analogous to Fig. 1 of Thompson and Solomon (2002), which examined 30-year linear trends for the period 1969-1998 see Fig. 20. We will update the record and extend the analysis to linear and non-linear trends.
2. Comparison of zonally averaged plots of trends in the vertical and horizontal components of the EP flux at 65S as a function of pressure and time. This is analogous to Fig. 4 of Christiansen (2001) see Fig. 21. The EP flux would be additionally separated into its planetary and synoptic wave contributions.
3. Comparison of zonally averaged plots of trends in the vertical component of the EP flux at 65S and 300 and 30 hPa as a function of time, which is equivalent to the total EP flux divergence above 300 and 30 hPa respectively (that is, the total wave driving at higher altitudes). This is analogous to Fig. 1 of Orr et al. (2013) see Fig. 22.
4. Identify sudden changes in EP fluxes which have caused any discrepancies or biases in the reanalyses (Lu et al., 2014).

**Concerns:** The comparison period of 1979-present includes the past decade during which the summertime SAM has been less markedly positive compared to the 1990s (see <http://www.nerc-bas.ac.uk/public/icd/gjma/newsam.sum.pdf>). Hence, it could be the marked downward propagation apparent in Thompson and Solomon (2002), who examined the period 1969-1998, is less obvious. This could be particularly problematic when examining trends in wave driving, as this is already typically a noisy field in reanalyses. An alternative could be to examine difference plots between seasons with SAM positive phase and SAM negative phase.

**Fig. 1.** 30-year (1969–98) linear trends in temperature (T, left) and geopotential height (Z, right) averaged over the radiosonde stations listed in Table 1. Trends are plotted as a function of calendar month and vertical level. Contours are drawn at 40 m per 30 years (–60, –20, 20 ...) and 1 K per 30 years (–1.5, –0.5, 0.5, ...). Dashed contours denote geopotential height and temperature decreases. Shading denotes trends that exceed 1 SD of the respective monthly time series.

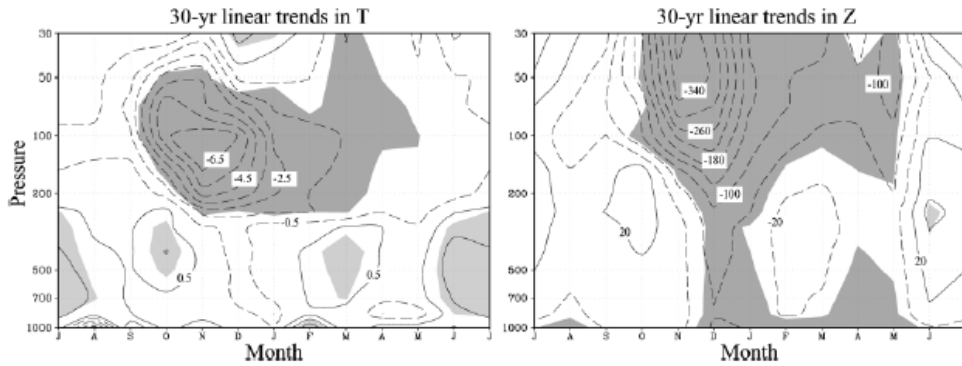
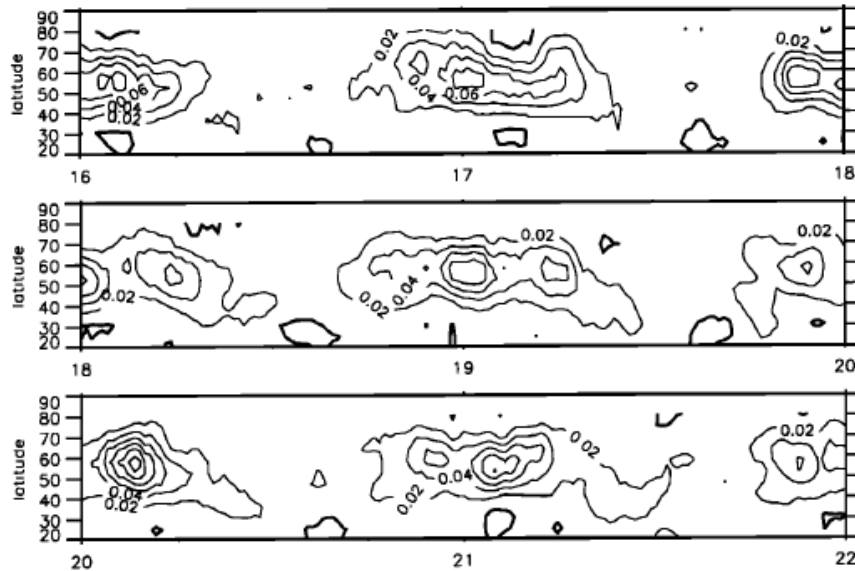


Figure 20: This plot is taken from Thompson and Solomon (2002). We will repeat this for all reanalyses, but for the period 1979-present. We will also examine the representation of the mean and variance between reanalyses.



**Figure 4.** The vertical component of the Eliassen-Palm flux  $F^z/\rho_0$  ( $\text{m}^2 \text{s}^{-2}$ ) at 100 hPa as function of time and latitude for the same 6 years as in Figure 2. The first and second plots are the NCEP reanalysis and the model, respectively. The data have been low-pass filtered to suppress timescales shorter than 30 days.

Figure 21: This plot is taken from Christiansen (2001). We will repeat this for all reanalyses, but examining the trend for the period 1979-present. We will also examine the representation of the horizontal component of the EP flux.

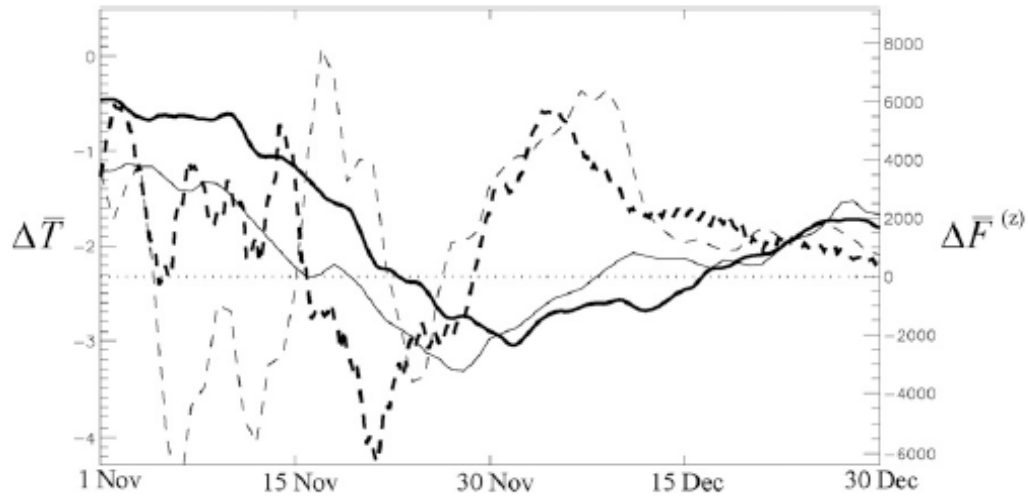


FIG. 1. Simulated (thick lines) and reanalysis (thin lines) daily changes of zonally averaged temperature  $\Delta\bar{T}$  averaged from 300 to 30 hPa and from  $60^{\circ}$  to  $80^{\circ}$ S (solid lines) and zonally averaged vertical EP flux  $\Delta\bar{F}^{(z)}$  at 30 hPa averaged from  $40^{\circ}$  to  $80^{\circ}$ S (dashed lines). Simulated changes are the 24-yr averaged differences between the ozone-hole and the pre-ozone-hole model runs. Reanalysis changes are ERA-40 23-yr linear trends (1979–2001). The units for the simulated (reanalysis) changes are  $\text{K} (\text{K decade}^{-1})$  for  $\Delta\bar{T}$  and  $\text{m}^3 \text{s}^{-2} (\text{m}^3 \text{s}^{-2} \text{decade}^{-1})$  for  $\Delta\bar{F}^{(z)}$ . Latitudinal (vertical) averages are area (height) weighted.

Figure 22: This plot is taken from Orr et al. (2013). We will repeat this for all reanalyses, but focusing on the trend and for the period 1979-present.

## 5.2 Trends in extreme events (Son)

Long-term trend of stratospheric extreme events. This will need to be integrated with Section 3. Fig. 23 illustrates the analysis in JRA-25 and several NCEP reanalyses.

**Other General References:** Karpechko et al. (2010a); Orr et al. (2012); Randel and Wu (1999); Solomon et al. (2010); Son et al. (2008, 2010)

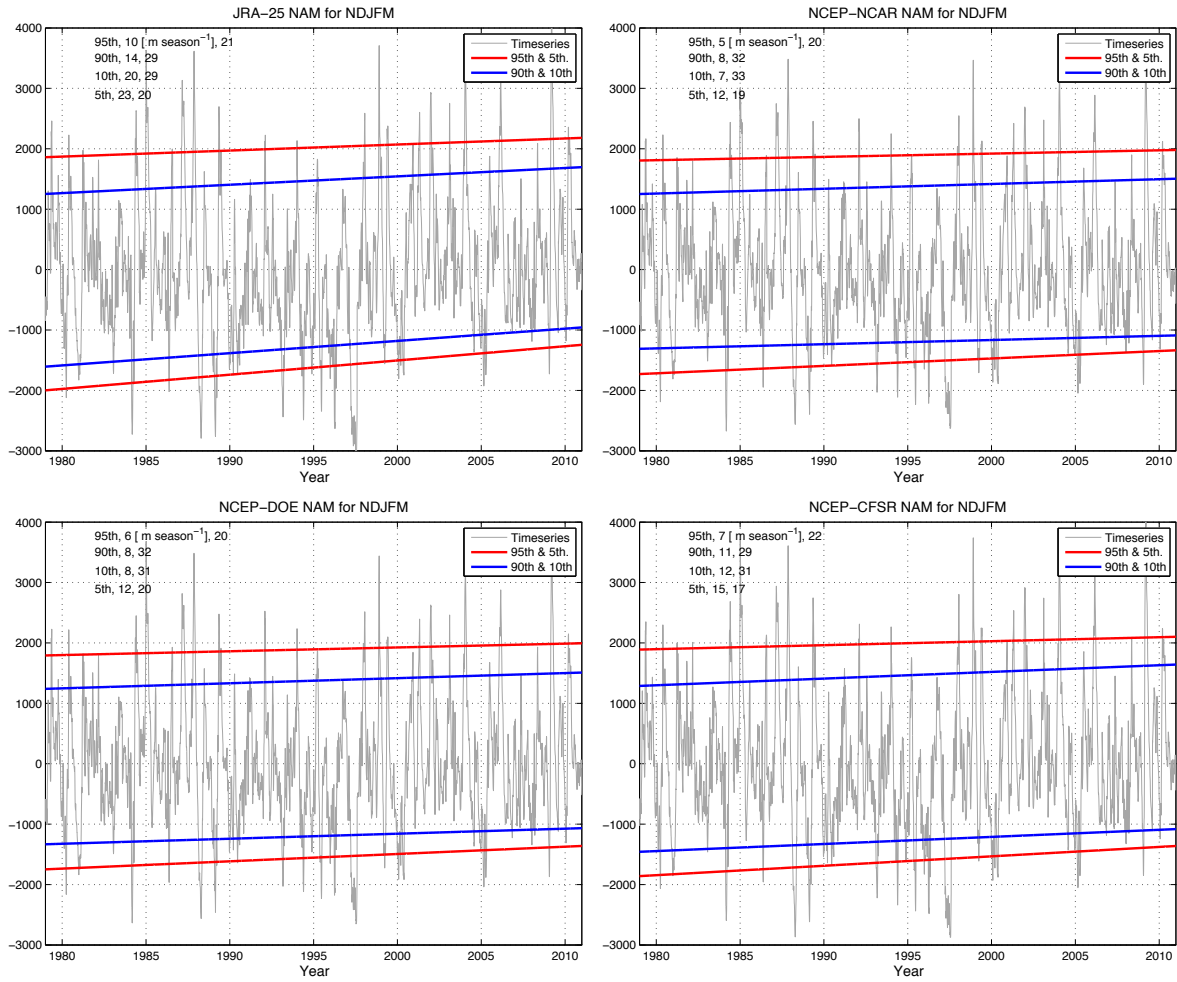


Figure 23: Temporal evolution of NDJFM NAM-index anomalies at 10 hPa for JRA25, NNR1, NNR2, and NNR3. The linear regressions for the 5th and 95th percentile (red) and 10th and 90th percentile (blue) are denoted with thick solid lines, and their trends are indicated on the top right corner of each plot (second column).

## **6 Summary and Conclusions**

I'll be excited when we're ready to write this...

## References

- Ayarzagüena, B., U. Langematz, and E. Serrano, 2011: Tropospheric forcing of the stratosphere: A comparative study of the two different major stratospheric warmings in 2009 and 2010. *J. Geophys. Res.*, **116**, doi:10.1029/2010JD015023.
- Baldwin, M. P. and T. Birner, 2013: On the stratospheric plunger... *t.b.d.*
- Baldwin, M. P. and T. J. Dunkerton, 1999: Propagation of the the Arctic Oscillation from the stratosphere to the troposphere. *J. Geophys. Res.*, **104**, 30 937–30 946.
- Baldwin, M. P. and T. J. Dunkerton, 2001: Stratospheric harbingers of anomalous weather regimes. *Science*, **294**, 581–584.
- Baldwin, M. P., D. B. Stephenson, D. W. J. Thompson, T. J. Dunkerton, A. J. Charlton, and A. O’Neill, 2003: Stratospheric memory and skill of extended-range weather forecasts. *Science*, **301**, 636–640.
- Barriopedro, D. and N. Calvo, 2014: On the relationship between enso, stratospheric sudden warmings, and blocking. *J. Climate*, **27**, 4704–4720, doi:10.1175/JCLI-D-13-00770.1.
- Barriopedro, D., R. Garcia-Herrera, and R. M. Trigo, 2010: Application of blocking diagnosis methods to General Circulation Models. Part I: A novel detection scheme. *Climate Dyn.*, **35**, 1373–1391, doi:10.1007/s00382-010-0767-5.
- Butchart, N., et al., 2011: Multimodel climate and variability in the stratosphere. *J. Geophys. Res.*, **116**, D05 102, doi:10.1029/2010JD014995.
- Butler, A. H., D. J. Seidel, S. C. Hardiman, N. Butchart, T. Birner, and A. Match, 2014: Defining sudden stratospheric warmings. *Bull. Am. Meteor. Soc.*, submitted.
- Cagnazzo, C. and E. Manzini, 2009: Impact of the stratosphere on the winter tropospheric teleconnections between ENSO and the North Atlantic and European Region. *J. Climate*, **22**, 1223–1238.
- Calvo, N., R. Garca, W. J. Randel, and D. R. Marsh, 2010: Dynamical mechanism for the increase in tropical upwelling in the lowermost tropical stratosphere during warm ENSO events. *J. Atmos. Sci.*, **67**, 2331–2340.
- Calvo, N., M. A. Giorgetta, R. Garcia-Herrera, and E. Manzini, 2009: Nonlinearity of the combined warm ENSO and QBO effects on the Northern Hemisphere polar vortex in MAECHAM5 simulations. *J. Geophys. Res.*, **114**, D13 109, doi:10.1029/2008JD011445.
- Charlton, A. J. and L. M. Polvani, 2007: A new look at stratospheric sudden warmings. Part I: Climatology and modeling benchmarks. *J. Climate*, **20**, 449–469.
- Charlton, A. J., et al., 2007: A new look at stratospheric sudden warmings. Part II: Evaluation of numerical model simulations. *J. Climate*, **20**, 470–488.

- Charlton-Perez, A. J., et al., 2013: On the lack of stratospheric dynamical variability in low-top versions of the CMIP5 models. *J. Geophys. Res.*, **118**, 2494–2505, doi:10.1002/jgrd.50125.
- Christiansen, B., 2001: Downward propagation of zonal mean zonal wind anomalies from the stratosphere to the troposphere: Models and reanalyses. *J. Geophys. Res.*, **106(D21)**, 27 307–27 322.
- Cnossen, I., H. Lu, C. J. Bell, L. J. Gray, and M. M. Joshi, 2011: Solar signal propagation: The role of gravity waves and stratospheric sudden warmings. *J. Geophys. Res.*, **116**, D02 118, doi:10.1029/2010JD014535.
- Crooks, S. A. and L. J. Gray, 2005: Characterization of the 11-year solar signal using a multiple regression analysis of the ERA-40 dataset. *J. Climate*, **18**, 996–1015.
- Driscoll, S., A. Bozzo, L. J. Gray, A. Robock, and G. Stenchikov, 2012: Coupled Model Inter-comparison Project 5 (CMIP5) simulations of climate following volcanic eruptions. *J. Geophys. Res.*, **117**, doi:10.1029/2012JD017607.
- Frame, T. H. A. and L. J. Gray, 2010: The 11-yr solar cycle in ERA-40 data: An update to 2008. *J. Climate*, **23**, 2213–2222.
- García-Herrera, R., N. Calvo, R. R. Garcia, and M. A. Giorgetta, 2006: Propagation of ENSO temperature signals into the middle atmosphere: A comparison of two general circulation models and ERA-40 reanalysis data. *J. Geophys. Res.*, **111**, D06 101, doi:10.1029/2005JD006061.
- Garfinkel, C. I. and D. L. Hartmann, 2007: Effects of the El-Niño Southern Oscillation and the Quasi-Biennial Oscillation on polar temperatures in the stratosphere. *J. Geophys. Res.*, **112**, D19112, doi:10.1029/2007JD008481.
- Gerber, E. P., et al., 2010: Stratosphere-troposphere coupling and annular mode variability in chemistry-climate models. *J. Geophys. Res.*, **115**, D00M06, doi:10.1029/2009JD013770.
- Hardiman, S. C., et al., 2011: Improved predictability of the troposphere using stratospheric final warmings. *J. Geophys. Res.*, **116**, doi:10.1029/2011JD015914.
- Hitchcock, P., T. G. Shepherd, and G. L. Manney, 2013: Statistical characterization of arctic polar-night jet oscillation events. *J. Climate*, in press.
- Ho, C.-H., H.-S. Kim, J.-H. Jeong, and S.-W. Son, 2009: Influence of stratospheric quasi-biennial oscillation on tropical cyclone tracks in the western North Pacific. *Geophys. Res. Lett.*, **36**, L06 702, doi:10.1029/2009GL037163.
- Ineson, S. and A. A. Scaife, 2009: The role of the stratosphere in the European climate response to el Niño. *Nature Geoscience*, **2**, 32–36, doi:10.1038/NGEO381.
- Karpechko, A. Y., N. P. Gillett, M. Dall’Amico, and L. J. Gray, 2010a: Southern Hemisphere atmospheric circulation response to the El Chichón and Pinatubo eruptions in coupled climate models. *Quart. J. Roy. Meteor. Soc.*, **136**, 1813–1822, doi:10.1002/qj.683.

- Karpechko, A. Y., N. P. Gillett, L. J. Gray, and M. Dall'Amico, 2010b: Influence of ozone recovery and greenhouse gas increases on Southern Hemisphere circulation. *J. Geophys. Res.*, **115**, doi:10.1029/2010JD014423.
- Limpasuvan, V., D. W. J. Thompson, and D. L. Hartmann, 2004: The life cycle of the northern hemisphere sudden stratospheric warmings. *J. Climate*, **17**, 2584–2596.
- Lu, H., T. J. Bracegirdle, T. Phillips, and J. Turner, 2014: Uncertainties in estimating wave forcing from reanalysis data sets: A comparative study of ERA-40 and ERA-Interim. *J. Climate*, submitted.
- Lu, H., C. Franzke, O. Martius, M. J. Jarvis, and T. Phillips, 2013: Solar wind dynamic pressure effect on planetary wave propagation and synoptic-scale Rossby wave breaking. *J. Geophys. Res.*, doi:10.1002/jgrd.50374.
- Lu, H., L. J. Gray, M. P. Baldwin, and M. J. Jarvis, 2009: Life cycle of the QBO-modulated 11-year solar cycle signals in the Northern Hemispheric winter. *Quart. J. Roy. Meteor. Soc.*, **135**, 1030–1043.
- Manzini, E., M. A. Giorgetta, M. Esche, L. Kornbluh, and E. Roeckner, 2006: The influence of sea surface temperatures on the northern winter stratosphere: Ensemble simulations with the MAECHAM5 model. *J. Climate*, **19**, 3863–3881.
- Martineau, P. and S.-W. Son, 2013: Planetary-scale wave activity as a source of varying tropospheric response to stratospheric sudden warming events: A case study. *J. Geophys. Res. Atm.*, doi:10.1002/jgrd.50871.
- Martineau, P. and S.-W. Son, 2014: Onset of circulation anomalies during stratospheric vortex weakening events: The role of planetary-scale waves. *J. Climate*, submitted.
- Martius, O., L. M. Polvani, and H. C. Davies, 2009: Blocking precursors to stratospheric warming events. *Geophys. Res. Lett.*, L14806, doi:10.1029/2009GL038776.
- Mitchell, D. M., A. J. Charlton-Perez, and L. J. Gray, 2011: Characterizing the variability and extremes of the stratospheric polar vortices using 2D moment analysis. *J. Atmos. Sci.*, **68**, 1194–1213.
- Mitchell, D. M., L. J. Gray, J. Anstey, M. P. Baldwin, and A. J. Charlton-Perez, 2013: The influence of stratospheric vortex displacements and splits on surface climate. *J. Climate*, **26**, 2668–2682, doi:10.1175/JCLI-D-12-00030.1.
- Nakamura, N. and A. Solomon, 2011: Finite-amplitude wave activity and mean flow adjustments in the atmospheric general circulation. Part i: Quasigeostrophic theory and analysis. *J. Atmos. Sci.*, **68**, 2783–2799, doi:10.1175/2011JAS3685.1.
- Newman, P. A., E. R. Nash, and J. E. Rosenfield, 2001: What controls the temperature of the Arctic stratosphere during spring? *J. Geophys. Res.*, **106**, 19 999–20 010.

- Nishii, K., H. Nakamura, and T. Miyasaka, 2009: Modulations in the planetary wave field induced by upward-propagating Rossby wave packets prior to stratospheric sudden warming events: A case-study. *Quart. J. Roy. Meteor. Soc.*, **135**, 39–52, doi:10.1002/qj.359.
- Orr, A., T. J. Bracegirdle, J. S. Hosking, W. Feng, H. K. Roscoe, and J. D. Haigh, 2013: Strong dynamical modulation of the cooling of the polar stratosphere associated with the Antarctic ozone hole. *J. Climate*, **26**, 662–668.
- Orr, A., T. J. Bracegirdle, J. S. Hosking, T. Jung, J. D. Haigh, T. Phillips, and W. Feng, 2012: Possible dynamical mechanisms for Southern Hemisphere climate change due to the ozone hole. *J. Atmos. Sci.*, **69**, 2917–2932.
- Randel, W. J. and F. Wu, 1999: Cooling of the Arctic and Antarctic polar stratospheres due to ozone depletion. *J. Climate*, **12**, 1467–1479.
- Seppälä, A., H. Lu, M. A. Clilverd, and C. J. Rodger, 2013: Geomagnetic activity signatures in wintertime stratosphere-troposphere temperature, wind. *J. Geophys. Res.*, doi:10.1002/jgrd.50236.
- Smith, K. L. and P. J. Kushner, 2012: Linear interference and the initiation of extratropical stratosphere-troposphere interactions. *J. Geophys. Res.*, **117**, doi:10.1029/2012JD017587.
- Solomon, S., K. H. Rosenlof, R. W. Portmann, J. S. Daniel, S. M. Davis, T. J. Sanford, and G.-K. Plattner, 2010: Contributions of stratospheric water vapor to decadal changes in the rate of global warming. *Science*, **327**, 1219–1223.
- Son, S.-W., et al., 2008: The impact of stratospheric ozone recovery on the Southern Hemisphere westerly jet. *Science*, **320**, 1486–1489, doi: 10.1126/science.1155939.
- Son, S.-W., et al., 2010: The impact of stratospheric ozone on Southern Hemisphere circulation change: A multimodel assessment. *J. Geophys. Res.*, **115**, D00M07, doi:10.1029/2010JD014271.
- Song, Y. and W. A. Robinson, 2004: Dynamical mechanisms for stratospheric influences on the troposphere. *J. Atmos. Sci.*, **61**, 1711–1725.
- Thompson, D. W. J. and T. Birner, 2012: On the linkages between the tropospheric isentropic slope and eddy fluxes of heat during Northern Hemisphere winter. *J. Atmos. Sci.*, **69**, 1811–1823, doi:10.1175/JAS-D-11-0187.1.
- Thompson, D. W. J., J. C. Furtado, and T. G. Shepherd, 2006: On the tropospheric response to anomalous stratospheric wave drag and radiative heating. *J. Atmos. Sci.*, **63**, 2616–2629.
- Thompson, D. W. J. and S. Solomon, 2002: Interpretation of recent Southern Hemisphere climate change. *Science*, **296**, 895–899.

- Thompson, D. W. J. and J. M. Wallace, 2000: Annular modes in the extratropical circulation. Part I: Month-to-month variability. *J. Climate*, **13**, 1000–1016.
- Wei, K., W. Chen, and R. Huang, 2007: Association of tropical Pacific sea surface temperatures with the stratospheric Holton-Tan Oscillation in the Northern Hemisphere winter. *Geophys. Res. Lett.*, **34**, L16 814, doi:10.1029/2007GL030478.
- Zubiaurre, I. and N. Calvo, 2012: The El Nino-Southern Oscillation (ENSO) Modoki signal in the stratosphere. *J. Geophys. Res. Atm.*, **117**, doi:10.1029/2011JD016690.